The Factors Behind the Morphotropic Phase Boundary in Piezoelectric Perovskites

ARTICLE *in* THE JOURNAL OF PHYSICAL CHEMISTRY B · JUNE 2009

Impact Factor: 3.3 · DOI: 10.1021/jp9024987 · Source: PubMed

THE JOURNAL OF PHYSICAL CHEMISTRY B LETTERS

XXXX, xxx, 000

The Factors Behind the Morphotropic Phase Boundary in Piezoelectric Perovskites

J. Frantti,*,† Y. Fujioka,† J. Zhang,‡ S. C. Vogel,‡ Y. Wang,‡ Y. Zhao,‡ and R. M. Nieminen†

Department of Applied Physics, Helsinki University of Technology, FI-02015-HUT Finland, and Los Alamos Neutron Science Center, Los Alamos National Laboratory, Los Alamos, New Mexico 87545

Received: March 19, 2009; Revised Manuscript Received: May 1, 2009

The best piezoelectric materials are solid solutions in the vicinity of the steep morphotropic phase boundary (MPB) separating rhombohedral and tetragonal phases in the composition−temperature plane. A classical example is the lead zirconate titanate [$Pb(Zr_xTi_{1-x})O_3$, PZT] system, with $x \approx 0.52$, where the two phases are separated by a boundary extending from the lowest temperatures up to several hundred degrees. The origin of the boundary has been under keen studies for 40 years. Recent interest is largely due to the need to develop new, lead-free piezoelectrics, for which a natural starting point is to understand the properties of the present systems. Here, we demonstrate, through high-pressure (up to 8 GPa) neutron powder diffraction experiments and density functional theory computations on lead titanate ($PbTiO_3$, PT), that it is the competition between two factors which determines the MPB. The first is the oxygen octahedral tilting, giving advantage for the rhombohedral *R*3*c* phase, and the second is the entropy, which in the vicinity of the MPB favors the tetragonal phase above 130 K. If the two factors are in balance over a large temperature range, a steep phase boundary results in the pressure−temperature plane.

Introduction

Piezoelectric applications, such as the atomic force microscope cantilever moving the tip in a presicely controlled manner on a sample surface, are often based on solid solutions in the vicinity of the phase boundary. An example is the phase boundary between the tetragonal and rhombohedral perovskite phases in the $Pb(Zr_xTi_{1-x})O_3$ (PZT) system, where $x \approx 0.52$. Due to the first-order phase boundary, rather small changes in the pressure or electric field results in a large response. For a stable performance, it is an advantage to have an almost vertical boundary in the composition−temperature plane; in the case of PZT, the boundary extends from the lowest temperatures up to 500 K, whereas the corresponding change in x is only about 0.03. This phase boundary is frequently termed the morphotropic phase boundary (MPB).[1] In solid solutions, the MPB is characterized by two competing, coexisting phases. However, the factors responsible for the vertical line are not well understood, and there has been considerable interest toward systems possessing a MPB. Notably, the monoclinic phase observed in the PZT system has been under keen studies as it often suggested that it explains the large electromechanical response near the MPB compositions via the polarization rotation model. However, solid solutions are somewhat difficult systems to study as the local disorder obscures the determination of the structure, not to mention the resulting difficulties in first-principles computations. Correspondingly, many high-pressure studies were dedicated to a more simple but isostructural $PbTiO_3$ (PT).[2−7] The early Raman scattering study reported a room-temperature continuous-phase transition between the ferroelectric and paraelectric phases to occur at 12.1 GPa,[2] consistent with the synchrotron X-ray diffraction studies.[3,4]

Hydrostatic pressure mimics the "chemical pressure" due to the cation substitution (such as Zr for Ti in PZT) and also eliminates complications due to the configurational entropy. Density functional theory (DFT) computations predicted a first-order phase transition to appear between the *P*4*mm* and *R*3*c* phases at $T = 0$ K at around $P = 9$ GPa of pressure.[7] Analogously to the case of PZT, this type of transition would be characterized by two-phase coexistence. On the basis of the high-pressure X-ray synchrotron diffraction study, the symmetry of PT at 22 GPa of pressure and 10 K was assigned to be rhombohedral,[5] which suggests that there would be a similar MPB in PT in the $P-T$ plane as that found in PZT in the $x-T$ plane. The transition between the *P*4*mm* and rhombohedral phases was interpreted to occur via monoclinic phases; however, this assignment is questioned in ref 8. For clarity, we note that a monoclinic symmetry, commonly observed in solid solution systems, does not mean that piezoelectric properties can be understood by the polarization rotation model (see, for instance, ref 9). According to a more recent X-ray synchrotron study, the room-temperature phase transformation sequence was reported to possess only tetragonal, (pseudocubic) tetragonal, and tetragonal structures with tilted oxygen octahedra, with no MPB.[6] This suggests that attention should be paid to the influence of temperature on phase stabilities. Since X-rays do not allow a reliable determination of the oxygen positions or octahedral tilts, neutrons are necessary. Octahedra tilting occurs often in perovskites as it allows energy minimization by changing the bond lengths and angles. Most clearly, the effect is seen in the case of low-symmetry rhombohedral phases, $R\bar{3}c$ and its subgroups since the octahedral tilting resulting in changes in bond lengths and angles is accompanied by an efficient

* To whom correspondence should be addressed. E-mail: johannes.frantti@hut.fi.
† Helsinki University of Technology.
‡ Los Alamos National Laboratory.

10.1021/jp9024987 CCC: $40.75

ohio2/yjp-yjp/yjp-yjp/yjp99907/yjp7541d07z | xppws | 23:ver.3 | 5/6/09 | 18:13 | Msc: jp-2009-024987 | TEID: mlk00 | BATID: jp6b147

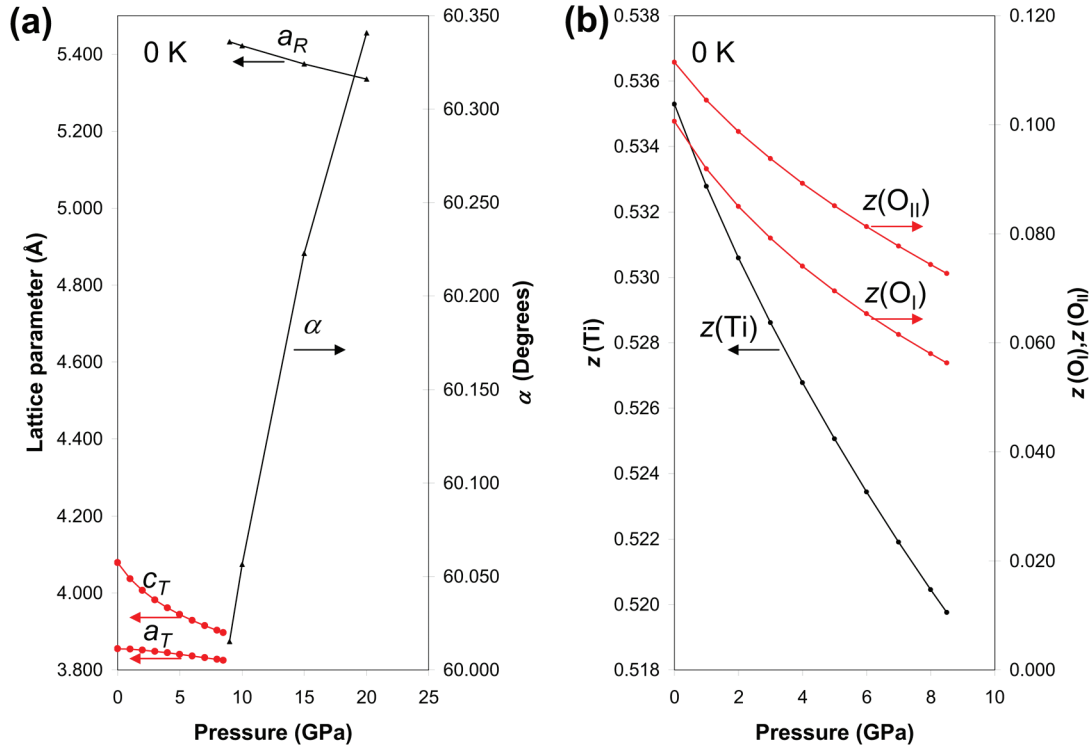

Figure 1. The structural parameters from the first-principles computations as a function of hydrostatic pressure at 0 K. (a) Tetragonal a_T and c_T and rhombohedral a_R and α lattice parameters and (b) the fractional coordinates of the titanium and oxygen ions in the *P*4*mm* phase; the lead ion was fixed at the origin, titanium was at (1/2, 1/2, z_{Ti}), and the oxygen ions were at (1/2, 1/2, z_{OI}), (1/2, 0, 1/2 + z_{OII}) and (0, 1/2, 1/2 + z_{OII}).

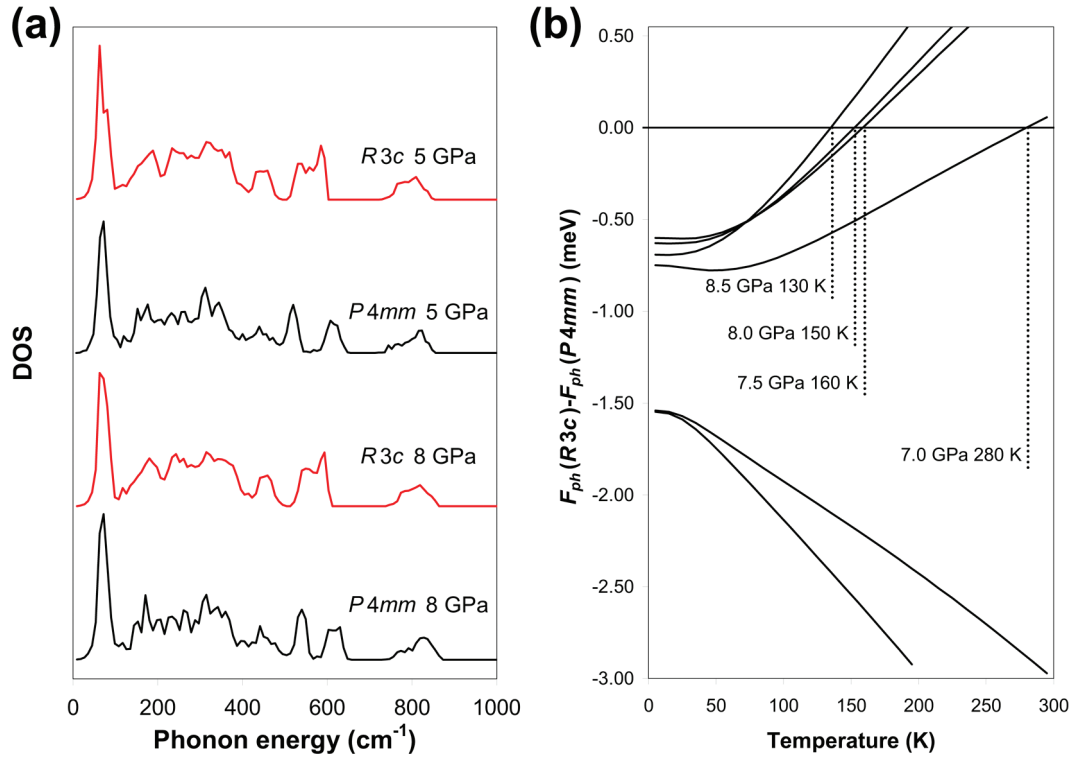

Figure 2. (a) Phonon densities of states of the *P*4*mm* and *R*3*c* phases at 5 and 8 GPa pressures. (b) The phonon free-energy difference between the *R*3*c* and *P*4*mm* phases as a function of temperature at fixed pressures. It is seen that phonon entropy favors the *P*4*mm* phase at elevated temperatures in the vicinity of the phase boundary. The lowest and second lowest curves correspond to 5 and 6 GPa pressure data.

volume compression.[10] The present study was dedicated to study the phase stabilities as a function of temperature and pressure. The DFT computations correspond to the 0 K temperature, and thus, the thermal energy must be separately estimated. Our hydrostatic high-pressure neutron powder diffraction studies and the first-principles DFT computations reveal that temperature plays an important role. As we show, the Gibbs energy $G = U - TS + PV$ contains two competing terms, determining the phase boundary in the $P-T$ plane; the entropy term TS favors the tetragonal structure at the phase boundary at elevated temperatures, whereas the pressure P times volume V term favors the oxygen octahedral tilting of the rhombohedral phase.

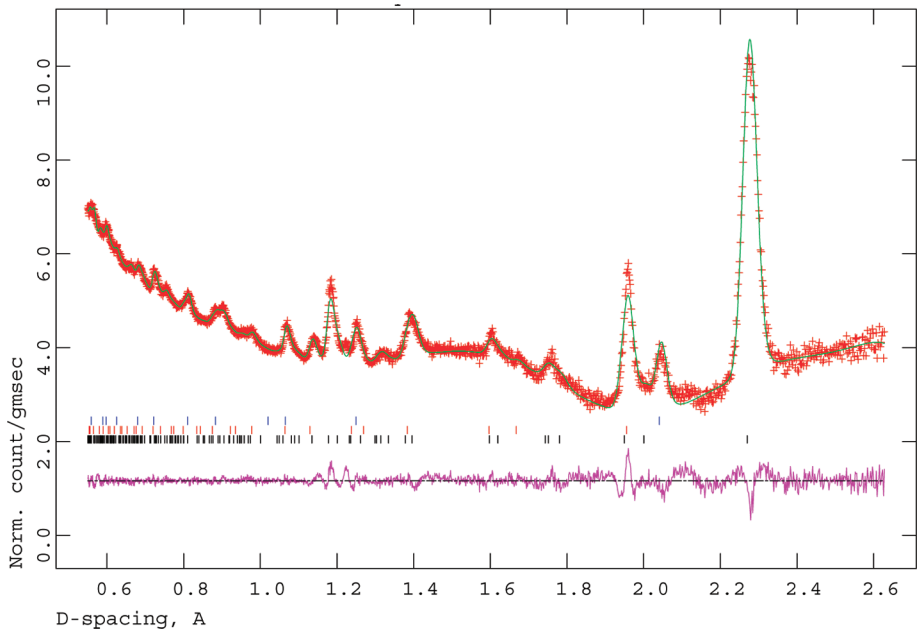

Figure 3. Observed and calculated neutron powder diffraction profiles and the corresponding difference curves at 600 K under 2.4 GPa of hydrostatic pressure. The tick marks, from top to bottom, are from the diamond anvils, NaCl pressure calibrant, and tetragonal $PbTiO_3$. The goodness-of-fit parameter $\chi^2 = 3.383$ (total for two histograms) and the residuals were $wR_p = 1.64, 2.26\%$, $wR_{pb} = 1.00, 1.75\%$, $R_p = 3.57, 3.92\%$, and $R_{pb} = 1.39, 2.49\%$, for the first and second histograms, respectively. Definitions for the parameters are given in the GSAS manual[15] on pages 166−168.

In the case of insulators, the phonon contribution to the internal energy U and the entropy S is significant at finite temperatures.

Methods Section

Lead titanate powder was prepared through the solid-state reaction technique by mixing the PbO and TiO_2 oxides in desired proportions. The phase purity and crystal structure were checked by X-ray powder diffraction measurements. High-pressure neutron powder diffraction experiments were carried out at the Los Alamos Neutron Scattering Center using the toroidal anvil press (TAP-98) equipment[11,12] set on the high-pressure-preferred orientation (HIPPO) diffractometer.[13,14] Pressure was generated using the high-pressure anvil cells. Sodium chloride was used as a pressure calibrant material. Data were collected at 300 and 600 K as a function of pressure. Rietveld refinements were carried out using the program General Structure Analysis System (GSAS).[15] The pressure was estimated from the reflection positions of the NaCl phase through the equation of state[16] up to 4 GPa. At higher pressures, no signal from the NaCl crystals was observed, and the pressure was estimated through the equation of state, based on the Birch−Murnaghan equation,[17,18] of $PbTiO_3$ reported in ref 3. It was necessary to include the reflections from the diamond anvils at high pressures in the refinement model. Typically, data sets from data banks 2 and 3 were used in order to get better statistics. The advantage of neutron diffraction over the X-ray diffraction is its ability to detect oxygen positions, which is a crucial factor when possible oxygen octahedral tiltings are studied.

The density functional theory code ABINIT[19,20] was used to compute the total energies, phonon frequencies and eigenvectors,[21] and the phonon entropies for tetragonal and rhombohedral phases at different hydrostatic pressures. We have earlier considered other space group symmetries and found the *P*4*mm* → *R*3*c* → $R\bar{3}c$ phase transformation chain to be the most favorable one at 0 K temperature, with the transition pressures at 9 and 27 GPa, correspondingly.[7,22] We tested the *Cmm*2, *Cm*, *Pm*, *I*4*cm*, and *R*3*m* symmetries and found that they had higher enthalpy values and often also phonon instabilities in the vicinity of the transition pressure.[7,8] Thus, the computationally expensive phonon contributions to the entropy and internal energy as a function of temperature were dedicated to the *P*4*mm* and *R*3*c* phases between 5 and 8.5 GPa of pressures. The computations were carried out within the standard local density approximation[23] and using a plane wave basis. Norm-conserving pseudopotentials were generated using the OPIUM package.[24] The estimation of the phonon contribution necessitates that a subset of k points within the Brillouin zone be selected and the corresponding eigenvalues (phonon energies) be computed. The phonon frequencies were computed by using the nonshifted 6 × 6 × 6 k point mesh (with the gamma point included) for the *P*4*mm* and the 4 × 4 × 4 for the *R*3*c* phase. For the phonon entropy and density-of-state computations, additional frequencies were estimated at intermediate k points through the Fourier interpolation scheme. Within the harmonic approximation, the temperature-dependent changes in internal energy and entropy were estimated.[25] We note that though the temperature dependences of the internal energy, entropy, or equilibrium volume are not solely determined by the phonons, it explains, to a first approximation, the temperature-dependent behavior of insulators. The computations must be limited to the pressures at which no phonon instabilities exist.

Ground-State Phases

Figure 1 shows the tetragonal and rhombohedral lattice parameters at 0 K as a function of hydrostatic pressure, as obtained from the DFT computations. In the tetragonal phase, the characteristic feature is the fast decrease of the c-axis parameter, which was also observed in experiments.[4] It is seen that the distortion from the centrosymmetric structure decreases with increasing pressure. Earlier computations showed that, also, the spontaneous polarization diminishes with increasing pressure.[7] It was reported that at room temperature, synchrotron measurements revealed weak superlattice reflections at 47 GPa[3] and above 43 GPa.[6] As noted

ohio2/yjp-yjp/yjp-yjp/yjp99907/yjp7541d07z | xppws | 23:ver.3 | 5/6/09 | 18:13 | Msc: jp-2009-024987 | TEID: mlk00 | BATID: jp6b147

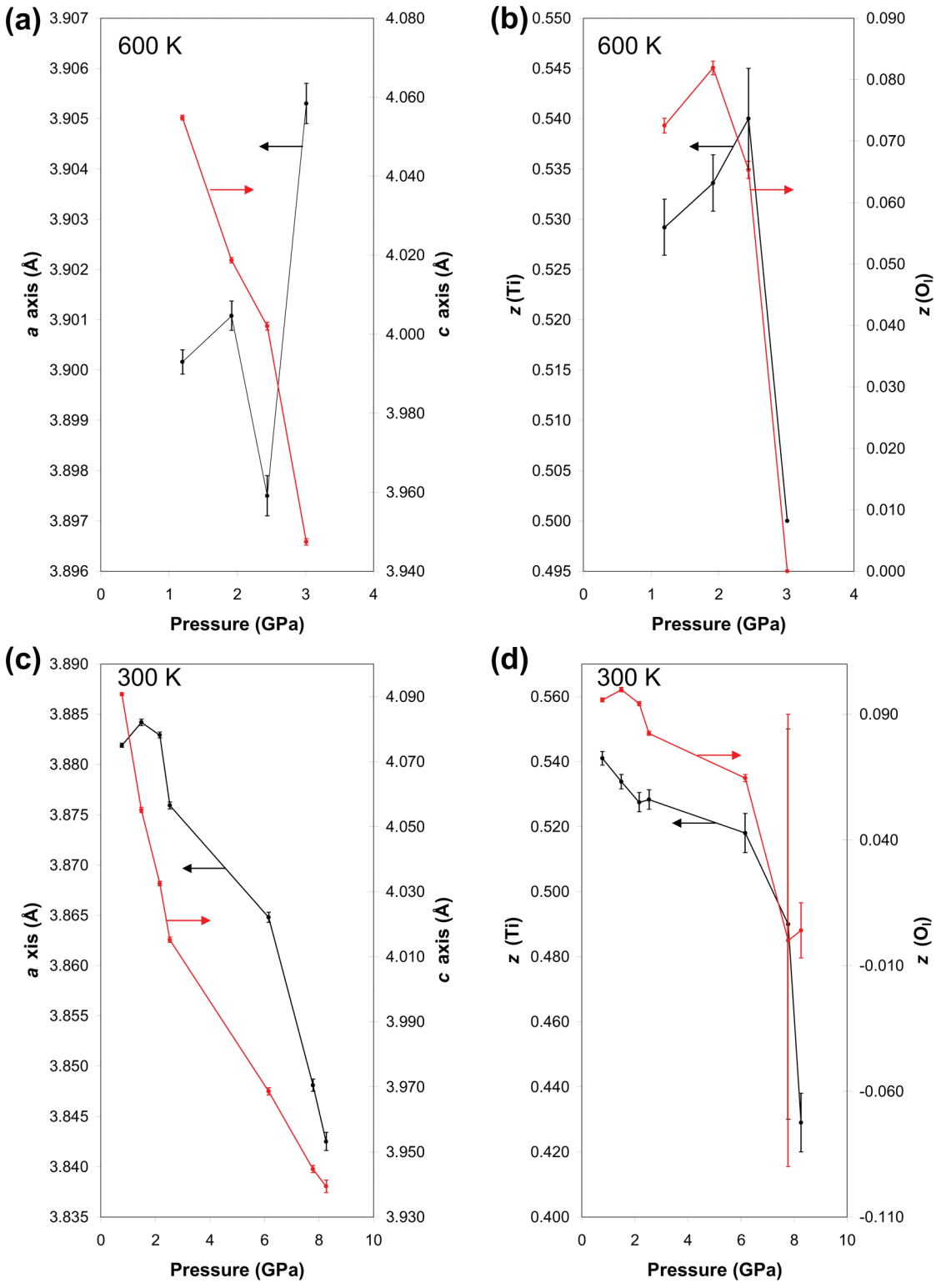

Figure 4. Tetragonal *a* and *c* lattice parameters and the fractional coordinates of the titanium and oxygen ions at 600 and 300 K as a function of hydrostatic pressure. Space group *P*4*mm* was used in the refinements. The lead ion was fixed at the origin, titanium was at (1/2, 1/2, z_{Ti}), and the oxygen ions were at (1/2, 1/2, z_O), (1/2, 0, 1/2 + z_O), and (0, 1/2, 1/2 + z_O) (here, a constraint $z_{OI} = z_{OII} = z_O$ was used). In the case of the highest-pressure structure at 600 K, all ions were relaxed to the inversion symmetry positions. Correspondingly, we switched to use the higher-symmetry space group *P*4/*mmm* for which the ion positions are fixed by symmetry.

above, the *I*4*cm* phase was not found to correspond to the minimum enthalpy at 0 K when $P \leq 40$ GPa. These reflections were assigned to the oxygen octahedra tilting in ref 6. This pressure range is beyond the one discussed in the present study, which focuses on the lowest-pressure phase boundary. At 0 K, the *R*3*c* phase was found to be energetically favorable above 9 GPa due to the more efficient compression allowed by the oxygen octahedra tilting, which can largely be understood by considering the Madelung energy term.[7] These results were confirmed by computing the enthalpies and phonon instabilities and phonon symmetries, which were remarkably consistent.

ohio2/yjp-yjp/yjp-yjp/yjp99907/yjp7541d07z | xppws | 23:ver.3 | 5/6/09 | 18:13 | Msc: jp-2009-024987 | TEID: mlk00 | BATID: jp6b147

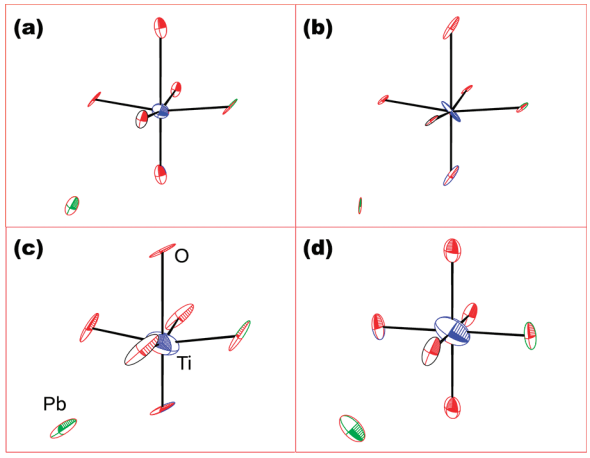

Figure 5. Atomic displacement ellipsoids (a) at 300 K and 0.8 GPa of pressure, (b) at 300 K and 2.5 GPa of pressure, (c) at 300 K and 8.3 GPa of pressure, and (d) at 600 K and 3 GPa of pressure. The tendency of oxygen ions to move along the ⟨101⟩ directions is clearly observed. Also, the elongation of the Ti displacement ellipsoid is clear and is similar to the well-known displacements of Pb ions. This demonstrates the crucial role that oxygen octahedra tilts play.

Competition between the Oxygen Octahedra Tilting and Phonon Entropy

The phonon density of state (DOS) of the *P*4*mm* and *R*3*c* phases is shown in Figure 2. It is seen that the low-frequency parts of the DOS functions are similar, which suggests that at lowest temperatures (where only the lowest-energy states are occupied), the phonon contribution does not favor one phase over the other. However, the phonon contribution to the Helmholtz free energy (which consists of the contributions to the internal energy and entropy) has an important role for the phase stability. At 5 GPa of pressure, the enthalpy difference between the rhombohedral and tetragonal phases was 5 meV,[7] whereas the phonon contribution is less than 3 meV when the temperature is below 200 K and is thus not able to drive a phase transition. Above 7.5 GPa, the phonon contribution can no longer be neglected as the competing phases have equal enthalpies, and thus, small differences can favor one phase over the other. This is the case as the *P*4*mm* phase is favored over the *R*3*c* phase above 130 K at 8.5 GPa of pressure. Since the differences between the enthalpy of competing phases were found to be rather large outside of the phase transition region, the phonon entropy behavior is clear; at elevated temperatures, the phase transition pressure between tetragonal and rhombohedral phases is pushed toward higher pressures.

High-Pressure Neutron Powder Diffraction Analysis at 300 and 600 K

At ambient conditions, PT is tetragonal, possessing a space group *P*4*mm*. Our Rietveld refinements showed that the structure could well be refined by the prototype perovskite structure up to 2.5 GPa pressures, after which structural parameters became unreasonable; oxygen octahedra were anomalously deformed, the Ti−O distances were unreasonable, and many of the isotropic and anisotropic titanium and oxygen atomic displacement parameters (ADP) became physically meaningless. Anisotropic and isotropic ADP parameters and linear absorption corrections were tested after the isotropic ADP parameters alone were found inadequate. Absorption corrections and ADP parameters were refined alternatively since their effect on diffraction intensities are similar. At high pressures, many oxygen diagonal ADP parameters remained negative. Negative principal ADP parameters are often a sign of an incorrect structural model. In addition, the absorption due to the high-pressure chamber can affect the intensities. It is well-known that in many Pb-based perovskite oxides, the Pb ions are often significantly displaced from their ideal sites, which is assigned to the $6s^2$ lone electron pair. This results in large ADP parameters for Pb. Also, the anomalous behavior of Ti ADP parameters is seen already at ambient pressures at low temperatures.[26] However, other Pb-based perovskites, such as PZT, did not reveal anomalous oxygen ADP parameters.[27,28] Since no signs of space group symmetry lowering were found and the use of subgroups (e.g., *I*4*cm*) did not eliminate the problem, we finally decided to use the anisotropic ADP parameters with no symmetry constraints (this was done by using the *P*1 symmetry, by constraining the nuclei positions to correspond to the *P*4*mm*, and by setting no constraints to ADP parameters) and to constrain the displacements of oxygen along the *c*-axis to be the same. For simplicity, absorption correction was not refined. This model worked very well and gave reasonable structural parameters. Figure 3 shows a typical refinement. The lattice parameters and ionic positions as a function of pressure at 300 and 600 K are given in Figure 4. We note that they are similar to the structural parameters at 0 K (compare to Figure 1).

Though the ADP ellipsoids must be adopted with caution, we note that they were elongated along the ⟨101⟩ directions; see Figure 5. This again reveals that the oxygen octahedral tilting is still an important mechanism at the elevated temperatures, though it is no more able to turn the structure to rhombohedral within the pressure range studied. The *I*4*cm* symmetry corresponds to the octahedra tilting in the *ab* plane, which in turn would suggest ADP ellipsoids elongated toward the ⟨110⟩ directions, in contrast to our observations. Synchrotron X-ray radiation experiments suggested that at room temperature, the *P*4*mm* phase transforms to a pseudocubic phase at 12 GPa,[6] though the detailed determination of the oxygen octahedra tilting through X-ray diffraction is often rather difficult. Our NPD data show that at high pressures, the oxygen displacements are anomalous, which offers an explanation for the reported deviations from the ideal cubic symmetry.[6] We propose that also the aforementioned anomalous behavior of Ti ADP parameters as a function of temperature is related to this competition and explains the deviations from the ideal cubic or tetragonal. The DFT computations[7] revealed the unstable octahedral tilting modes, which strongly supports the experimental observations.

Conclusions

Our high-pressure neutron powder diffraction experiments and first-principles computations demonstrate that the phase boundary in the temperature−pressure plane is largely determined by the two competing factors, oxygen octahedra tilting allowing efficient compression and phonon entropy favoring the tetragonal phase. The first mechanism dominates at the lowest temperatures, whereas the entropy term dictates at elevated temperatures. Neutron powder diffraction data show that both mechanisms coexist even above room temperature at high pressures. If the two terms balance in the large temperature range at (nearly) constant pressure, a steep morphotropic phase boundary results. In the case of practical applications, on the basis of solid solutions, composition plays the role of pressure, and the configurational entropy term due to the substitutional disorder cannot be neglected.

ohio2/yjp-yjp/yjp-yjp/yjp99907/yjp7541d07z | xppws | 23:ver.3 | 5/6/09 | 18:13 | Msc: jp-2009-024987 | TEID: mlk00 | BATID: jp6b147

Acknowledgment. This project was supported by the Academy of Finland (Projects 207071, 207501, 214131, and the Center of Excellence Program 2006-2011). The Finnish IT Center for Science (CSC) is acknowledged for providing computing resources. This work has benefited from the use of the Lujan Neutron Scattering Center at LANSCE, which is funded by the U.S. Department of Energy's Office of Basic Energy Sciences. Los Alamos National Laboratory is operated by Los Alamos National Security LLC under DOE contract DE-AC52-06NA25396.

References and Notes

(1) Jaffe, B.; Cook, W. R; Jaffe, H. *Piezoelectric Ceramics*; Academic Press: London, 1971.

(2) Sanjurjo, J. A.; Lṕez-Cruz, E.; Burns, G. *Phys. Rev. B* **1983**, *28*, 7260.

(3) Ming, L. C.; Shieh, S. R.; Kobayashi, Y.; Endo, S.; Shimomura, O.; Kikegawa, T. *Geophys. Monogr.* **1998**, *101*, 441.

(4) Sani, A.; Hanfland, M.; Levy, D. *J. Solid State Chem.* **2002**, *167*, 446.

(5) Ahart, M.; Somayazulu, M.; Cohen, R. E.; Ganesh, D. P.; Mao, H.; Russell, J.; Hemley, J.; Ren, Y.; Liermann, P.; Wu, Z. *Nature* **2008**, *451*, 545.

(6) Janolin, P.-E.; Bouvier, P.; Kreisel, J.; Thomas, P. A.; Kornev, I. A.; Bellaiche, L.; Crichton, W.; Hanfland, M.; Dkhil, B. *Phys. Rev. Lett.* **2008**, *101*, 237601.

(7) Frantti, J.; Fujioka, Y.; Nieminen, R. M. *J. Phys. Chem. B* **2007**, *111*, 4287.

(8) Frantti, J.; Fujioka, Y.; Nieminen, R. M. *J. Phys.: Condens. Matter* **2008**, *20*, 472203.

(9) Kisi, E. H.; Forrester, J. S. *J. Phys.: Condens. Matter* **2008**, *20*, 1.

(10) Thomas, N. W.; Beitollahi, A. *Acta Crystallogr.* **1994**, *B50*, 549.

(11) Zhao, Y.; Von Dreele, R. B.; Morgan, J. G. *High Pressure Res.* **1999**, *16*, 161.

(12) Zhao, Y.; He, D.; Qian, J.; Pantea, C.; Lokshin, K. A.; Zhang, J.; Daemen, L. L. Development of high P−T neutron diffraction at LANSCE - toroidal anvil press, TAP-98, in the HIPPO diffractometer. In *Advances in High-Pressure Technology for Geophysical Applications*; Chen, J., Wang, Y., Duffy, T. S., Shen, G., Dobrzhinetskaya, L. P. , Eds.; Elsevier Science & Technology: New York, 2005; pp 461−474.

(13) Wenk, H.-R.; Lutterotti, L.; Vogel, S. *Nucl. Instrum. Methods Phys. Res., Sect. A* **2003**, *515*, 575.

(14) Vogel, S. C.; Hartig, C.; Lutterotti, L.; Von Dreele, R. B.; Wenk, H.-R.; Williams, D. J. *Powder Diffr.* **2004**, *19*, 65.

(15) Larson, A. C.; Von Dreele R. B. *General Structure Analysis System. LANSCE MS-H805*; Los Alamos National Laboratory: Los Alamos, NM, 2000.

(16) Decker, D. L. *J. Appl. Phys.* **1971**, *42*, 3239.

(17) Birch, F. *Phys. Rev.* **1947**, *71*, 809.

(18) Murnaghan, F. D. *Am. J. Math.* **1937**, *59*, 235.

(19) Gonze, X.; Beuken, J.-M.; Caracas, R.; Detraux, F.; Fuchs, M.; Rignanese, G.-M.; Sindic, L.; Verstraete, M.; Zerah, G.; Jollet, F.; Torrent, M.; Roy, A.; Mikami, M.; Ghosez, Ph.; Raty, J.-Y.; Allan, D. C. *Comput. Mater. Sci.* **2002**, *25*, 478.

(20) Gonze, X.; Rignanese, G.-M.; Verstraete, M.; Beuken, J.-M.; Pouillon, Y.; Caracas, R.; Jollet, F.; Torrent, M.; Zerah, G.; Mikami, M.; Ghosez, Ph.; Veithen, M.; Raty, J.-Y.; Olevano, V.; Bruneval, F.; Reining, L.; Godby, R.; Onida, G.; Hamann, D. R.; Allan, D. C. *Z. Kristallogr.* **2005**, *220*, 558.

(21) Gonze, X. *Phys. Rev. B* **1997**, *55*, 10337.

(22) Our phase transition sequence is different from the one suggested in Ganesh, P.; Cohen, R. E. *J. Phys.: Condens. Matter* **2009**, *21*, 064225. which they dismissed by a note "We believe that the results by Frantti et al. are incorrect due to some technical error". This statement is unfounded; we checked the pseudopotentials and compiled newer version of the Abinit code, carried out computations again, and found no technical or other errors. The outcome was the same as that published in ref 7.

(23) (a) Perdew, J. P.; Zunger, A. *Phys. Rev. B* **1981**, *23*, 5048. (b) Perdew, J. P.; Wang, Y. *Phys. Rev. B* **1992**, *45*, 13244.

(24) Rappe, A. M.; Rabe, K. M.; Kaxiras, E.; Joannopoulos, J. D. *Phys. Rev. B* **1990**, *41*, 1227.

(25) Gonze, X.; Lee, C. *Phys. Rev. B* **1997**, *55*, 10355.

(26) Glazer, A. M.; Mabud, S. *Acta Crystallogr.* **1978**, *B34*, 1065.

(27) Corker, D. L.; Glazer, A. M.; Whatmore, R. W.; Stallard, A.; Fauth, F. *J. Phys.: Condens. Matter* **1998**, *10*, 6251.

(28) Frantti, J.; Ivanov, S.; Eriksson, S.; Rundlöf, H.; Lantto, V.; Lappalainen, J.; Kakihana, M. *Phys. Rev. B* **2002**, *66*, 064108.

JP9024987